

Paper surface modification by plasma deposition of double layers of organic silicon compounds†

Ing H. Tan,^a Maria Lucia P. da Silva^b and Nicole R. Demarquette*^a

^aEscola Politecnica da Universidade de São Paulo, Depto. de Engenharia Metalurgica e de Materiais, Av. Prof. Mello Moraes 2463, CEP 05508-900 São Paulo, S.P. Brasil.

E-mail: nick@usp.br

^bDepto. de Engenharia Eletrica, Av. Luciano Gualberto, no. 158 - trav. 3, 05508-900 São Paulo, SP Brazil

Received 8th October 2000, Accepted 18th January 2001

First published as an Advance Article on the web 27th February 2001

In this work, filter paper was coated with plasma depositions of hexamethyldisilazane (HMDS), and double layers of HMDS and *n*-hexane, and HMDS and tetraethyl orthosilicate (TEOS). In the case of double layers of HMDS and TEOS, TEOS deposition times of 2, 4 and 6 minutes were studied. The double layers were interfaced by an intermixing layer, in which both reagents were present. All coating films formed adhered well to the substrate, and resulted in water repellent paper surfaces with apparent water contact angles above 100 degrees and water adsorption around 15 g m⁻². Apparent water contact angles were not affected by immersion in strong basic and acid solutions, or by exposure to ultraviolet light for 106 hours. Water adsorption of HMDS, HMDS-*n*-hexane and HMDS-TEOS (6 min) coated samples was not significantly altered by these resistance tests, but HMDS-TEOS (2, 4 min) coated samples were hydrolysed by immersion in strong basic solution and by ultraviolet light. These results seemed to indicate that the HMDS-TEOS intermixing layer was fragile and malformed. This hypothesis was confirmed by Raman and atomic force microscopies, which showed heterogeneous structures with very high peaks, and by XPS analysis, which indicated oxidation of carbonic species and crosslinkings together with elimination of ethylene gas probably triggered in the intermixing layer. The porosity of paper was not altered showing that all depositions were conformal. FTIR analysis of HMDS coatings indicated that the films formed were crosslinked by ultraviolet light showing its potential for outdoor applications.

Introduction

The hydrophilic character of cellulose is a desirable property for some paper applications such as utilities, but is a problem for applications like liquid recipients, printing, or other applications where dimensional stability is important. It is known that in 50% relative humidity environments, cellulose adsorbs about 5% of its own weight of water.¹ Due to its fibre network structure, paper is a porous material, and can be covered by polymer films in order to make it impermeable to water. In some applications however, it is desirable that the system be permeable to air but water repellent. Therefore, making cellulose fibres hydrophobic can be interesting in applications such as printing with non-water based inks. Currently, water repellence is accomplished using solvents and organic reagents, mostly wax emulsions, quaternary ammonium salts and hydrophobic resin finishes, which require discarding and can cause environmental problems.²

Cold plasma processing is already a well known and widely used technique for etching and surface modification in the electronics industry. Plasmas create extremely reactive species like ions, free radicals and metastable species, which allow reactions to occur at much lower temperatures than in conventional methods, or even reactions that would not occur at all, if the reagents are not under plasma conditions. Low quantities of reagents are used and discarded in plasma processing since treatment times are very short (a few minutes

for deposition and even seconds in activation processes), and low pressures are used. Furthermore, low energies are used in most processes making them economically attractive.

Plasma polymerisation of hydrocarbon monomers like cyclohexane³ has been demonstrated to make cellulose surfaces hydrophobic. However, the treated paper in this case loses its porous structure due to the film's bridging over the fibres. Adhesion of these films to cellulose substrates was not tested, and some doubts exist as to whether the whole surface was covered. Furthermore, the ultraviolet light resistance and chemical resistance of the film have not been studied yet. Plasma polymerisation of carbon tetrafluoride⁴ and fluorine alkyl silanes^{5,6} have also been studied leading to high contact angles as a result of intense surface fluorination. However, the use of CFCs and other compounds containing fluorine is not an environmentally friendly process owing to the hazardous effects on, for example, the atmosphere's ozone layer.

Organic silicon compounds are commonly used for plasma depositions in microelectronics, optics and surface protection industries. One of their great advantages is the ease of manipulation, since they are liquids of low toxicity. Plasma deposition of hexamethyldisilazane (HMDS) presents interesting characteristics owing to: 1) the presence of Si-N-Si bonds, creating the possibility of forming silicone type structures and, 2) the presence of CH₃ groups which can modify the surface properties of the coated material making it hydrophobic. In a previous work,⁷ we demonstrated that HMDS films deposited in a low frequency plasma reactor produced hydrophobic films with high deposition rates (up to 6000 Å min⁻¹), high concentration of methyl radicals and good resistance to strong inorganic acids and bases. The presence of silicon in

†Electronic Supplementary information (ESI) available: atomic force micrograph and optical micrograph of HMDS-TEOS film (90 seconds deposition). See <http://www.rsc.org/suppdata/jm/b0/b008050k/>

the molecule and its strong affinity to the oxygen atom of cellulose is a strong indication that plasma deposited HMDS films will adhere to cellulose substrates very easily.

The objective of this work was to study the hydrophobic protection of paper that can be obtained by plasma deposition of HMDS, and by the deposition of a double layer of HMDS and tetraethyl orthosilicate (TEOS), or HMDS and *n*-hexane, with an intermixing layer in between. TEOS is the most common organic silicon compound used for plasma deposition of SiO₂ in microelectronics. Pyrolysis of TEOS has been known since the sixties,⁸ can occur at atmospheric or low pressures,⁹ but requires plasma assisted deposition to occur at low temperatures. The objective of mixing HMDS with TEOS was to produce an interpenetrated network of TEOS and HMDS polymers such as the one shown in Fig. 1, in which an oxynitride type film could be formed. These structures have Si–N–Si and Si–O–Si bonds, which are known to add mechanical and chemical resistance to the deposited film.¹⁰ Despite the presence of oxygen in the TEOS molecule, its ethylene groups would give water repellence. *n*-Hexane was chosen as a second reagent since it is easily polymerised in plasma conditions, requiring low energy and low reagent flux.¹¹ Deposition of *n*-hexane with HMDS was attempted to lower costs, with a first layer of HMDS functioning as an adhesion promoter. An HMDS–*n*-hexane interface layer is expected to have two polymers bonded either chemically (by Si–C bonds) or by van der Waals interactions. In both cases (TEOS or *n*-hexane), a two layer deposition was chosen since previous experiments¹² demonstrated deposition difficulties when two reagents were used simultaneously. Filter paper was chosen as the cellulose substrate since it is the most hydrophilic type of paper.

Adhesion of the film to the cellulose substrate was tested by measuring the apparent water contact angles before and after dipping in acid and basic solutions. The hydrophobic nature of the surface was measured by apparent water contact angles, and water adsorption was tested using the Cobb method. Chemical resistance to acids and bases, and ultraviolet resistance were also tested. Morphological modifications were investigated by scanning electron microscopy. The HMDS–TEOS double layer coatings were analysed by infrared spectroscopy (FTIR), Raman and atomic force (AFM) microscopy.

Materials and methods

The equipment used for plasma depositions was a parallel plate capacitively coupled reactor powered by a 40 kHz source. The reactor had two 20 cm diameter stainless steel electrodes, 3 cm apart, one of them grounded and used as substrate holder. Base

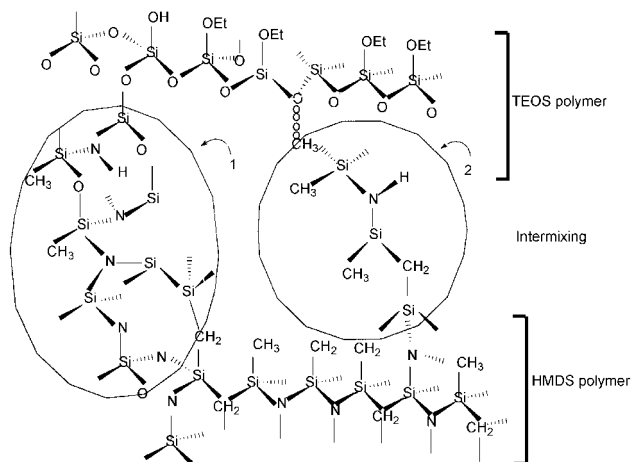


Fig. 1 Schematic visualisation of HMDS and TEOS double layer with an intermixing layer, which could have strong oxynitride structures (1) or entangled chains bound only by intermolecular forces (2).

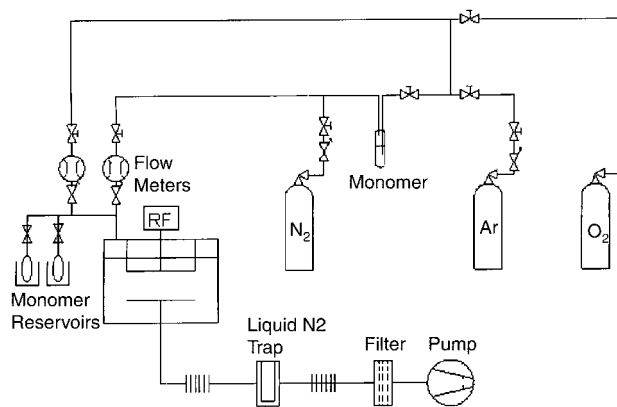


Fig. 2 Schematic diagram of the plasma reactor used.

pressures of 20 mTorr could be reached within a few minutes with a rotary pump. Monomers were injected by pressure gradient at room temperature, with the working pressure controlled by changing the aperture of the pumping valve, and consequently the pumping speed. Fig. 2 shows a schematic diagram of the reactor used.

Three types of depositions were made: 1) HMDS alone (called HMDS in the remainder of the text); 2) double layers of HMDS and TEOS (called TEOS_{*x*} in the remainder of the text, where *x* is the TEOS deposition time in minutes); 3) double layers of HMDS and *n*-hexane (called hexane in the remainder of the text). For double layered films, HMDS was first deposited for two minutes, after which the second monomer (TEOS or *n*-hexane) was injected simultaneously for 30 seconds (the intermixing period). The HMDS reservoir valve was then closed, and the second monomer deposition was made for 2, 4 and 6 minutes for TEOS and for 6 minutes for *n*-hexane.

The deposition conditions are presented in Table 1. Pressures of TEOS and *n*-hexane shown in this table are measured with plasma. Power during the intermixing period was gradually increased from 50 W to 90 W or 100 W. A profile meter (model Dektak 3030) was used to measure the step height when part of the wafer was covered during deposition, giving the film's thickness, and the deposition rates shown in the table.

Silicon wafers (<100>, p type, 10–20 Ω cm, 3 inches diameter) were used as substrates for profile meter, FTIR, Raman and AFM analysis. High purity filter paper with less than 0.007% ash content from Binzer & Munkell was used as cellulose substrate, in 5 cm × 5 cm samples. This type of paper was used because it does not contain non-cellulosic components. Therefore, the contact angles values reported here do not depend on surface chemical heterogeneity. The reagents used were HMDS (Hoescht, industrial use), high purity TEOS (Merck, for synthesis) and *n*-hexane (chromatographic grade).

Apparent water contact angles were measured using a Rame–Hart goniometer after each treatment, and after tests of ultraviolet light and chemical resistance. The accuracy of the measurement was ±2° and the dispersion of the data (five to six measurements were made for each sample in different positions) was around ±7°. Surfaces of paper sheets are far from ideal for contact angle measurement due to their topographical and chemical heterogeneity. It is well known that contact angles made by drops of liquids on a surface depend on the surface roughness and heterogeneity.¹³ Theore-

Table 1 Deposition conditions

| | Pressure/ mTorr | Power/ W | Deposition time/min | Deposition rate/Å min ⁻¹ |
|------------------|--------------------|-------------|------------------------|--|
| HMDS | 500 | 50 | 2 | 2200 |
| TEOS | 200 | 100 | 2, 4, 6 | 200 |
| <i>n</i> -Hexane | 600 | 90 | 6 | 300 |

tical treatments relating the apparent contact angles (formed by a drop of liquid on the surface of the material with a certain roughness) to real contact angles (formed by a drop of liquid on the ideally planar surface of the material) can be found in many textbooks although a precise relationship is difficult to evaluate. It can be demonstrated^{13,14} and has been shown experimentally¹⁵ that real contact angles are increased by surface roughness. In particular Shen *et al.*¹⁵ observed that water contact angles measured for sized single fibres are systematically smaller than those for sized paper sheets by about 20–30°. Measuring contact angles formed by drops of water of an unmodified filter paper is literally impossible as water penetrates the paper rapidly owing to its porous structure which makes it absorbent. We observed that the deposition of hexamethyldisilazane (HMDS) and double layers of HMDS and *n*-hexane, and HMDS and tetraethyl orthosilicate (TEOS) made the paper repellent to water and that stable drop forms were obtained to measure contact angles. Since the substrate on which the sessile drops of water were formed always had the same topography, as will be shown by scanning electron microscopy later in the paper, the values of apparent contact angle reported here can be used in a comparative way. They should neither be used as absolute values that reveal the chemistry of the surface nor be used to calculate the surface energy of the plasma treated paper. Other methods such as inverse gas chromatography¹⁶ are more appropriate to evaluate surface tension of heterogeneous structures. Water adsorption was tested using the Cobb method, which consists of placing a column of water on the treated paper for 20 minutes and measuring the water adsorbed by mass difference.

Adhesion and chemical resistance of the films formed by plasma deposition on the paper surface were tested by dipping the treated samples in solutions of NaOH (pH 14) and H₂SO₄ (pH 2.7) for a few seconds (for adhesion test) or during 15 minutes (for chemical resistance tests). Then, the apparent contact angles formed by drops of water, and water adsorption were measured again for comparison with the non-dipped samples. If not well adhered, the films would be interpenetrated by the solutions and would peel off.

The deposited hydrophobic layers are intended mainly to protect documents and other applications of paper used in indoor conditions. Therefore, resistance to ultraviolet light was tested exposing the treated samples to filtered UV light, according to the international standard ISO 105-B02. This is a test of colour fastness of textiles to artificial light (Xenon arc fading lamp test), which is representative of the effects of indoor ultraviolet light, to which documents are typically subjected, in contrast to the much harsher outdoor conditions. The samples were exposed for 8, 50 and 100 hours using a Hanau's Xenotest model 150 (1500 W of lamp power, with lamp-sample distance of 65 mm).

The morphological modifications on the paper surface were verified by scanning electron microscopy (Cambridge Instruments, Stereoscan 240), and the morphology of the films deposited on silicon wafers was observed using a Digital Instruments atomic force microscope model AFM-3 with a type-E scanner.

Chemical analysis of HMDS-TEOS double layer films was performed by Fourier Transform Infrared Spectroscopy (Bio-Rad's model QS-300), by X-ray Photoelectron Spectroscopy (Kratos Analytical model XSAM HS with a 1253,6 eV, 180 W MgK α radiation), and by Raman microscopy (Renishaw System 3000 with a He/Ne laser).

Results and discussion

Infrared spectra of films deposited on silicon wafers showed Si-CH₃ (850–840 cm⁻¹), N-H (1180–1175 cm⁻¹), Si-CH₂-Si (1090–1020 cm⁻¹) and Si-N-Si (900–830 cm⁻¹) bonds for

HMDS films,⁶ Si-O-Si (1050–1250 cm⁻¹), C-H_n (2960 cm⁻¹) and Si-OH (1650 cm⁻¹) bonds for TEOS films, and C-H_n bonds only for *n*-hexane depositions. HMDS-TEOS films spectra presented mainly HMDS species, as shown by the FTIR spectra of Fig. 3. This is probably due to the much thicker layer of HMDS, originating from a higher deposition rate (see deposition rates in Table 1). The only difference between the HMDS and HMDS-TEOS spectra occurred between 1300 cm⁻¹ and 1000 cm⁻¹ indicating the presence of Si-O-Si bonds.

Fig. 4 shows the apparent water contact angles and water adsorption of the treated samples. Apparent contact angles around 120° were measured for all cases. Recently Shen *et al.*¹⁵ proposed a possible way of correlating the apparent water contact angle to the real contact angle formed by a drop of water on a sheet of filter paper. For this they used the Cassie and Baxter¹⁷ equation that can be used to calculate the contact angle made by a drop of a liquid on a wire screen in which the wires occupy a fraction f_1 . According to Cassie and Baxter,¹⁷ if the drop of liquid makes a real contact angle θ_1 on the wire, then from eqn. (1) between θ_1 and θ_2 , the apparent contact angle can be obtained:

$$\cos \theta_2 = f_1 \cos \theta_1 - f_2 \quad (1)$$

Where

$$f_1 = 1 - f_2 \quad (2)$$

In order to infer f_1 and f_2 they used confocal laser-scanning microscopy. The values of (f_1, f_2) were respectively (0,47; 0,53) and (0,65;0,35) for a non-calendered sized filter paper and calendered sized filter paper respectively. Using eqn. (1) and the values reported by Shen *et al.*¹⁵ we can estimate that the real contact angles made by a drop of water on our paper surface were of the order of 85° showing water repellence. This value of 85° corroborates the values we obtained for silicon treated surfaces which are well known to be planar, since it follows the SEMI standard.

Water adsorption of around 15 g m⁻², a very good result for

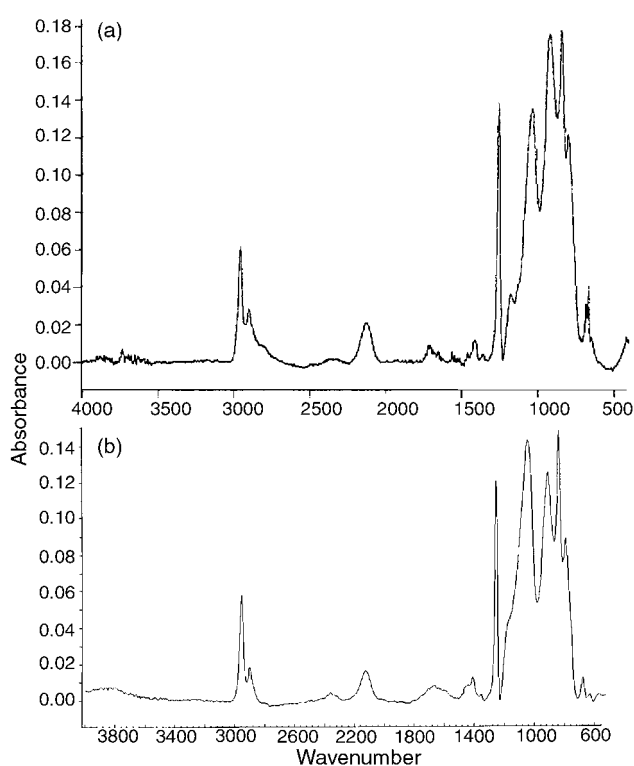


Fig. 3 FTIR spectrum of (a) HMDS and (b) HMDS-TEOS (3.5 min) films deposited on silicon wafers.

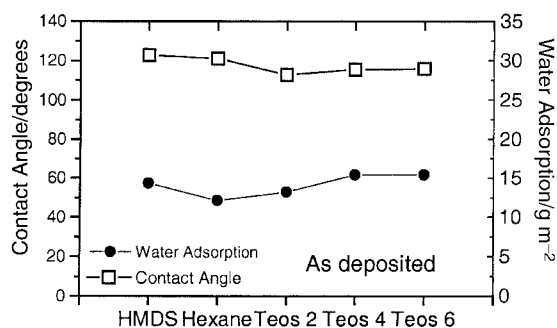


Fig. 4 Water contact angles and water adsorption of treated samples.

filter paper (untreated paper adsorbs normally around 80 g m^{-2}), showed that for all deposition conditions (reagents and time) the paper samples became water repellent.

The adhesion of the films to the substrate was tested by dipping the treated samples in the same acid and basic solutions for 5 seconds and measuring the apparent contact angles. It was still possible to measure an apparent contact angle as stable drop forms were still obtained. All apparent angles were unchanged (well above 90°) showing good adhesion of all films to the paper substrate, as expected.

Fig. 5 shows the apparent water contact angles and water adsorption after the treated samples had been immersed in a strong basic solution for 15 minutes. Water contact angles were not affected by the strong basic immersion. Water adsorption of all treated papers increased. This increase occurred to a lesser extent for HMDS and TEOS6 samples, while the TEOS2 sample gave the highest water adsorption. As will be explained later, this could be due to a defective TEOS layer exposing a reactive intermixing layer which was hydrolysed by the basic solution according to eqn. (3),

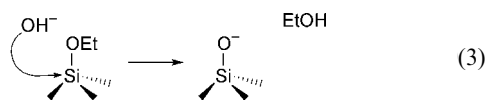


Fig. 6 shows the water apparent contact angles and water adsorption of the different samples after immersion in strong acid solution (H_2SO_4) for 15 minutes. It can be seen that in the case of HMDS and hexane both the water apparent contact angles and water adsorption remained the same. In the case of TEOS x (for $x=2, 4$ and 6 minutes) the water contact angles decreased slightly and water adsorption increased slightly most likely due to hydrolysis of the ethylene groups in the TEOS layer surface and the formation of Si-OH bonds (eqn. (3)).

Fig. 7 and 8 show the water apparent contact angles and water adsorption for the treated papers after UV exposure for different time duration. It can be seen in Fig. 7 that the apparent contact angles were not affected even after 106 hours of UV exposure. It can be seen from Fig. 8 that water adsorption: a) decreased for HMDS samples, probably due to

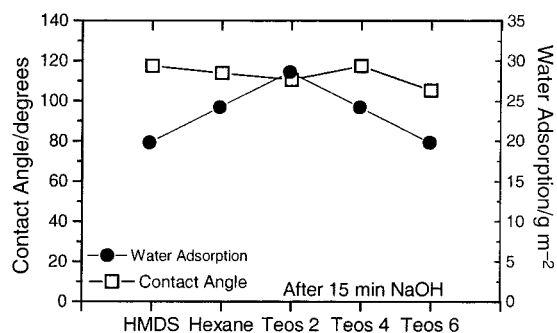


Fig. 5 Water contact angles and water adsorption of treated samples after immersion in strong basic solution.

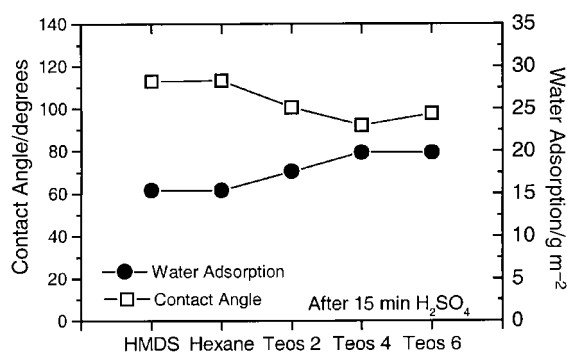
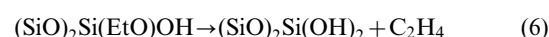
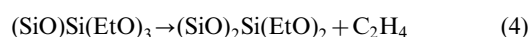


Fig. 6 Water contact angles and water adsorption of treated samples after immersion in strong acid solution.

crosslinking induced by UV light, b) remained constant for hexane and TEOS6 and c) increased considerably for TEOS2 and TEOS4. The increase of water adsorption for TEOS2 and TEOS4 samples indicates, as in the case of basic immersion, that a defective TEOS layer exposes a malformed and reactive HMDS-TEOS intermixing layer. In this case, the UV radiation is probably triggering the loss of ethylene groups by the mechanism shown in eqn. (4)–(6). A similar reaction is known to occur for SiO_2 films produced by TEOS deposition, which release gases by electron addition¹⁸ in the same way as in the pyrolysis of TEOS.¹⁹



This reaction mechanism is corroborated by XPS analysis done on the TEOS2 sample before and after UV exposure. Tables 2 and 3 show the atomic concentration and atomic composition analysis results respectively. The accuracy of the results is within 3–4%. It can be seen from Table 2 that the surface of TEOS2 after UV exposure is richer in O and poorer

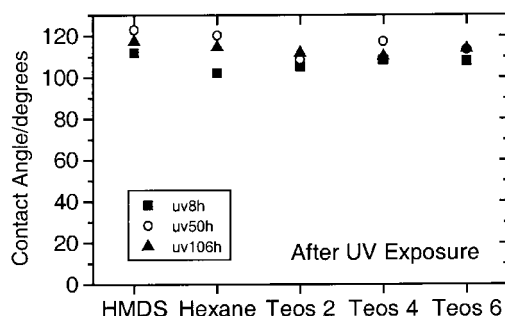


Fig. 7 Water contact angles of treated samples after exposure to UV light.

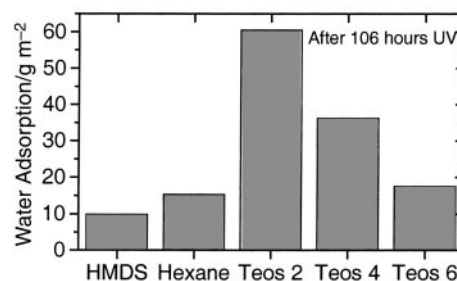


Fig. 8 Water adsorption of treated samples after 106 hours of UV exposure.

Table 2 Elemental composition and atomic ratios obtained by XPS

| | Atomic concentrations (%) | | | | Atomic ratios | |
|----------------------------|---------------------------|-----------------|------------------|-----------------|---------------|------|
| | C (284.8 eV) | O (532.5 eV) | Si (103.3 eV) | N (398.7 eV) | C/Si | O/Si |
| TEOS2 | 64.9 | 23.3 | 10.3 | 1.5 | 6.3 | 2.3 |
| TEOS2 after 106 h of UV | 48.0 | 38.6 | 13.4 | — | 3.6 | 2.9 |

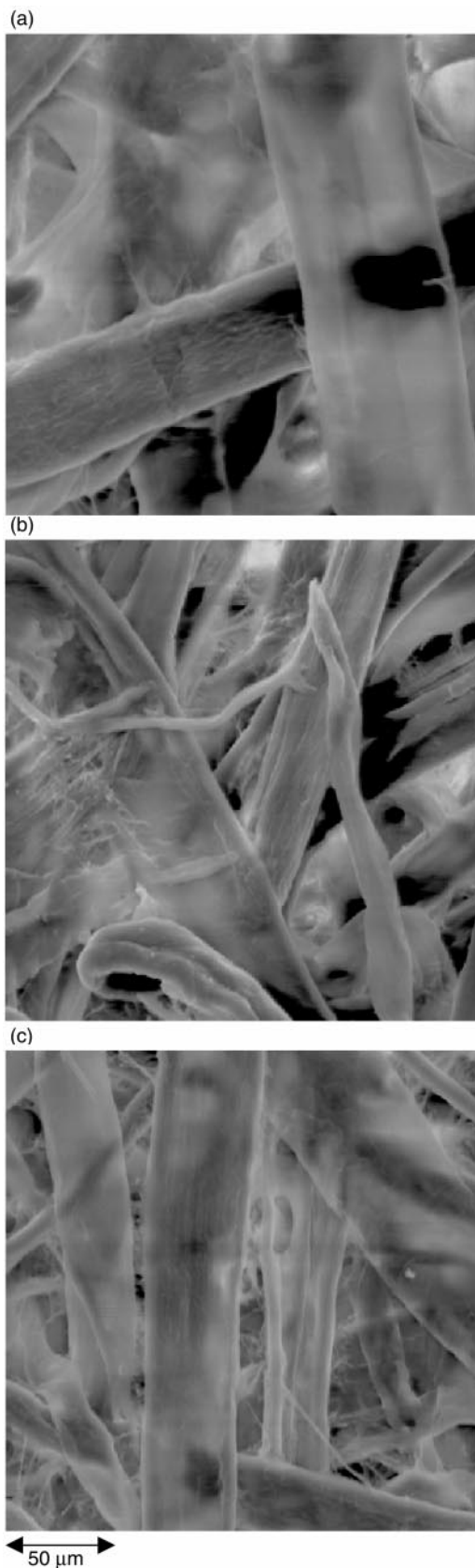
in C. It can be seen from Table 3 that oxidation occurs on carbonic species, with the formation of hydroxy and carbonyl groups. The amount of Si at the surface is constant within experimental error. This is due to the fact that it is not possible to lose silicon atoms by reaction in the film to form compounds in the gaseous state. These results are qualitatively in agreement with eqn. (4)–(6) presented above. Table 2 shows C/Si and O/Si for TEOS2 before and after UV exposure. It can be seen that the loss of C is proportionally much greater than the gain in O. Since oxidation of carbonic radicals should lead to the formation of C=O, C–OH and/or COOH, the carbon loss is better explained if the reactions triggered by the UV light occurred mainly by the elimination of C₂H₄ (eqn. (4)–(6)). It is probable that the reaction begins in the intermixing layer, which corresponds to the most stressed part of the film, and since the reaction does not need oxygen to occur. The decrease in Si–OH bonds shown in Table 3 indicates possible crosslinks by condensation reactions.

In order to understand the difference in the effects of the basic and UV resistance tests on the contact angles, which were unaltered, and water adsorption, which in some cases was altered, possible morphological modifications were investigated by scanning electron microscopy. Water adsorption is related not only to the hydrophobic character of the surface, as is water contact angle, but also to the porous structure of the paper, which could be affected by the plasma deposition. Fig. 9 (a to c) shows typical micrographs of the filter paper: a) before plasma treatment, b) after plasma treatment and c) after plasma treatment and UV exposure. TEOS2 is shown here because this sample showed the largest difference between contact angle results and water adsorption (see Fig. 7 and 8). It can be seen from the micrographs that the porosity of the paper was not affected by the plasma deposition or by the UV exposure. This can be explained by the fact that plasma deposition of these reagents is conformal, that is, it follows and does not affect the substrate's topography.

As already mentioned, water contact angle depends mainly on the surface chemistry and topography or roughness. Since topography was not altered and contact angle did not change with chemical and UV resistance tests, the surface chemistry must have remained mostly unaltered. XPS analysis of the worst TEOS2 case shows only a modest increase in oxidation of the carbonic radicals, which is partly compensated by a decrease in the highly hydrophilic Si–OH bonds, which

Table 3 Composition of carbon and silicon species of HMDS–TEOS (2 min) films before and after UV exposure

| Composition of atomic concentrations (%) | Composition of atomic concentrations (%) | |
|--|--|----------------------|
| | TEOS2 | TEOS2 after 106 h UV |
| Carbonic species | | |
| C–C, C–H (284.8 eV) | 77 | 65 |
| C–O (286.5 eV) | 19 | 24 |
| C=O (288.3 eV) | 4 | 11 |
| Silicon species | | |
| Si–O (103.3 eV) | 77 | 83 |
| Si–OH (101.7 eV) | 23 | 17 |

**Fig. 9** Scanning electron microscopy images of: (a) untreated filter paper, (b) filter paper treated with HMDS and (c) filter paper treated with HMDS–TEOS (2 min) after 106 hours of UV exposure.

crosslink turning into Si–O–Si bonds. As will be explained later, this chemical change probably comes from a defective TEOS layer exposing part of a degraded intermixing layer. The most reasonable explanation then, is that during the water adsorption test, the hydrostatic pressure resulted in the

penetration of water into the intermixing layer, which was malformed, with internal stresses and dangling bonds, favouring chemical reactions. This is corroborated by the fact that the sample with thinner TEOS layer (TEOS2) is more sensitive to the tests, while TEOS4 and TEOS6 samples, with progressively thicker TEOS layers, are correspondingly less affected.

A defective TEOS layer is likely to occur during the first minutes of deposition because the deposition rate of TEOS is much smaller than that of HMDS, so that the interface should be mainly formed by HMDS originated species. Furthermore, TEOS deposition chemistry is based on ionic species,²⁰ which are formed at higher energies.²¹ Since the reactor chamber was contaminated by HMDS for some time after its source has been shut off, not only the intermixing layer, but the first upper layers as well, will most probably present HMDS originated species. Therefore, the TEOS2 film probably still presented intermixing characteristics, formed by entangled polymeric chains of TEOS and HMDS (case 2 of Fig. 1), instead of oxynitride structures (case 1 of Fig. 1).

In order to study the intermixing layer, HMDS was deposited on a silicon wafer, followed by a 90 s deposition of TEOS and HMDS injected simultaneously. The FTIR spectrum of this film was similar to that of Fig. 3, and did not show bonds related to oxynitride structures. The film was analysed by Raman microscopy, which unlike FTIR, is capable of detecting non-polar groups, such as C=C bonds, which could appear with the decomposition of TEOS. Optical micrography of the film's surface showed that it is heterogeneous with pits and peaks. Chemical analysis of most peaks was not possible due to fluorescence, but C=C bonds were observed (in the detection limit) in some of them, while the film's base showed only CH_n bonds. The atomic force micrograph of the film shows peaks as high as 2100 Å, which surpass the TEOS layer thickness, especially in the case of 2 minutes of TEOS deposition (which should be around 400 Å), indicating that some of these islands could be exposed in the surface. The deposition mechanism consistent with these results is as follows: initially, TEOS is adsorbed in some active sites of the HMDS film and continually reacts in these sites owing to lack of compatibility with the HMDS film (probably owing to the highly polar Si-O bonds of the TEOS molecules attracting each other), and to a high reactivity of the islands formed, as indicated by the heterogeneous topography of these islands shown in an AFM micrograph. Unlike HMDS, whose deposition is based on neutrals,²² TEOS molecules are decomposed by the plasma into ions,²⁰ which are accelerated by the plasma sheath bombarding the substrate, and creating the pits observed. Bombardment of TEOS islands by TEOS ions with higher energy removes ethyl radicals creating new active sites necessary for the film's growth. On the other hand, TEOS ions with lower energy result in the decomposition of the film with the creation of C=C bonds. This is the most probable explanation for the C=C bonds observed, since active species of HMDS present during the intermixing period will take part of the available energy away from the TEOS ions. C=C bonds could not have been formed from HMDS originated species, since there has not been observed to date, any deposition condition that could result in the decomposition of HMDS forming this type of bond, including heating of the substrate, which only affects the deposition rate.

The decrease in water adsorption of the HMDS film exposed to UV light was an interesting result, and was investigated in more detail by depositing the same film on a silicon wafer and examining the FTIR spectrum before and after the sample was exposed to unfiltered ultraviolet light. The film was exposed to UVA light (a 22 W lamp, with a wavelength of 350 nm, distant 5 cm from the sample) for 20 hours and to UVC light (same parameters, but with a wavelength of 250 nm) for 5 hours. Table 4 shows the relative intensities of FTIR spectra obtained by exposure of HMDS films to UVA light, and Table 5 those

Table 4 Relative intensities of FTIR spectrum of HMDS film exposed to UVA light. $I(x/y)$ represents the relative peak heights between x and y species

| Relative intensities of FTIR spectrum | | | | |
|---------------------------------------|--------------------------------|------------------------------------|--|----------|
| $I(\text{Si-CH}_3/\text{Si-N-Si})$ | $I(\text{N-H}/\text{Si-N-Si})$ | $I(\text{Si-O-Si}/\text{Si-N-Si})$ | $I(\text{Si-CH}_2\text{-Si}/\text{Si-N-Si})$ | Time/min |
| 0.83 | 0.28 | — | 0.37 | 0 |
| 0.81 | 0.23 | — | 0.43 | 10 |
| 0.86 | 0.26 | — | 0.45 | 95 |
| 0.88 | 0.18 | Traces | 1.1 | 190 |
| 0.80 | 0.25 | Traces | 0.6 | 600 |
| 0.47 | 0.14 | Traces | 0.35 | 1200 |

Table 5 Relative intensities of FTIR spectrum of HMDS film exposed to UVC light. $I(x/y)$ represents the relative peak heights between x and y species

| Relative intensities of FTIR spectrum | | | | |
|---------------------------------------|--------------------------------|------------------------------------|--|----------|
| $I(\text{Si-CH}_3/\text{Si-N-Si})$ | $I(\text{N-H}/\text{Si-N-Si})$ | $I(\text{Si-O-Si}/\text{Si-N-Si})$ | $I(\text{Si-CH}_2\text{-Si}/\text{Si-N-Si})$ | Time/min |
| 0.81 | 0.27 | — | 0.44 | 0 |
| 0.86 | 0.27 | — | 0.76 | 15 |
| 0.88 | 0.23 | Trace | 0.93 | 75 |
| 0.96 | 0.23 | Trace | 1.16 | 275 |

obtained by exposure to UVB light. Similar results were obtained for both tests: Si-CH₂-Si bonds increased compared to Si-N-Si bonds, indicating that UV light favours crosslinks through carbon radical reactions. For UVA light a maximum in Si-CH₂-Si intensity was observed after 3 hours. However, the Si-CH₂-Si band showed traces of Si-O-Si bonds (both species have peaks in the same spectrum region) in both experiments, indicating that oxidation reactions occurred simultaneously. It should be noted that solar radiation consists mainly of UVA, some UVB and no UVC radiation. The fact that UVC, the most energetic of the three types of radiation, causes mainly crosslinkings after up to 3 hours of exposure, indicates that besides being resistant to indoor UV radiation, HMDS films could be used as a protective layer for paper in outdoor applications as well.

Conclusions

We have demonstrated that plasma deposition of hexamethyldisilazane (HMDS) is an efficient method for making paper surfaces hydrophobic, while still maintaining its porous structure. This deposition is resistant to strong bases and acids, as well as to indoor ultraviolet light. The deposition of a double layer of HMDS followed by *n*-hexane is an alternative which involves lower costs, resulting in a protection layer with the same characteristics as of HMDS alone. The HMDS layer functions in this case as an adhesion promoter of *n*-hexane to the cellulose substrate. A double layer of HMDS followed by TEOS resulted in a similar protection coating only for TEOS depositions longer than 6 minutes, and is therefore not recommended. The HMDS-TEOS intermixing layer did not result in an oxynitride structure, and may have resulted instead, in a more fragile, reactive and porous layer. The resistance of HMDS films to ultraviolet light through crosslinkings could make this process suitable for paper applications in more aggressive atmospheric conditions like outdoor panels.

Acknowledgements

We would like to thank the Laboratory of Molecular Spectroscopy of the Chemistry Institute of the University of São Paulo for the Raman Microscopy analysis. This work was supported by FAPESP (Fundação de Amparo à Pesquisa do Estado de São Paulo, process numbers 95/9287-0, 96/06947-2 and 97/06071-6).

References

- 1 J. Kroschwitz, in *Concise Encyclopedia of Polymer Science and Engineering*, Wiley & Sons, NY, 1990, p. 704.
- 2 A. M. Schwartz, in *Advances in Textile Processing*, ed. J. E. Lynn and J.J. Press, 1961, vol. 1, pp. 263–298.
- 3 X. Tu, R. A. Young and F. Denes, *Cellulose*, 1994, **1**, 87–106.
- 4 F. Denes, Z. Q. Hua, E. Barrios and R. A. Young, *J. Macromol. Sci.–Pure Appl. Chem.*, 1995, **A32**, 1405–1443.
- 5 A. Hozumi and O. Takai, *Thin Solid Films*, 1997, **303**, 222–225.
- 6 A. Hozumi, N. Kakinoki, Y. Asai and O. Takai, *J. Mater. Sci. Lett.*, 1996, **15**, 675–677.
- 7 S. Nogueira, M. L. da Silva and I. H. Tan *Proceedings of the 14th International Conference on Plasma Chemistry*, 1999, Praha, Czech Republic, vol. III, 1393.
- 8 L. L. Tedder, J. E. Crowell and M. A. Logan, *J. Vac. Sci. Technol., A*, 1991, **9**(3), 1002.
- 9 M. E. Bartram and H. K. Moffat, *J. Vac. Sci. Technol., A*, 1994, **12**(4), 1027.
- 10 R. González-Luna, M. T. Rodrigo, C. Jiménez and J. M. Martínez-Duart, *Thin Solid Films*, 1998, **317**, 347–350.
- 11 H. Yassuda, in *Plasma Polymerization*, Academic Press, New York, 1985, ch. 9.
- 12 I. H. Tan, N. Demarquette, M. L. da Silva, F. T. Degasperri and R. Dallacqua, *Proceedings of the 14th International Conference on Plasma Chemistry*, 1999, Praha, Czech Republic, vol. IV, 1907.
- 13 S. Wu, in *Polymer Interfaces and Adhesion*, ch. 1, Marcel Dekker, New York, 1982.
- 14 A. W. Adamson and A. P. Gast, in *Physical Chemistry of Surfaces*, 6th edition, Wiley Interscience, New York, 1997, pp. 358–361.
- 15 W. Shen, Y. Filonanko, Y. Truong, I. H. Parker, N. Brack, P. Pigram and J. Liesegang, *Colloids Surf., A*, 2000, **173**, 117–126.
- 16 M. N. Belgacem, G. Czeremuszkina, S. Sapielha and A. Gandini, *Cellulose*, 1995, **2**, 145.
- 17 A. B. D. Cassie and S. Baxter, *Trans. Faraday Soc.*, 1944, **40**, 546.
- 18 M. L. P. Silva, A. R. Cardoso and J. J. Santiago-Aviles, *Proc. Mater. Res. Soc. Symp.*, 1998, **500**, 97–100.
- 19 L. L. Tedder, G. Lu and J. E. Crowell, *J. Appl. Phys.*, 1991, **69**, 7037.
- 20 A. R. Cardoso, M. L. P. Silva and J. J. Santiago-Aviles, *Proc. Mater. Res. Soc. Symp.*, 1998, **500**, 93–96.
- 21 M. L. P. Silva and J. M. Riveros, *Int. J. Mass Spectrom. Ion Process*, 1997, **165**(166), 83–95.
- 22 F. Fracassi, R. d'Agostino, P. Favia and M. van Sambeck, *Plasma Sources Sci. Technol.*, 1993, **2**, 106–111.